Binding of ferrzdoxin to ferredoxin: NADP+ oxidoreductase: The role of carboxyl groups, electrostatic potential and molecular dipole moment

ARTICLE *in* PROTEIN SCIENCE · JULY 1993

Impact Factor: 2.85 · DOI: 10.1002/pro.5560020707 · Source: PubMed

Protein Science (1993), *2*, 1126–1135. Cambridge University Press. Printed in the USA.

Binding of ferredoxin to ferredoxin:NADP$^+$ oxidoreductase: The role of carboxyl groups, electrostatic surface potential, and molecular dipole moment

ANTONIO R. DE PASCALIS,[1] ILIAN JELESAROV,[1] FRIEDERIKE ACKERMANN,[1] WILLEM H. KOPPENOL,[2] MASAKAZU HIRASAWA,[3] DAVID B. KNAFF,[3] AND HANS RUDOLF BOSSHARD[1]

[1] Biochemisches Institut der Universität Zürich, Winterthurerstrasse 190, CH-8057 Zürich, Switzerland
[2] Department of Chemistry, Louisiana State University, Baton Rouge, Louisiana 70803-1804
[3] Department of Chemistry and Biochemistry, Texas Tech University, Lubbock, Texas 79409-1061

(RECEIVED January 22, 1993; REVISED MANUSCRIPT RECEIVED March 24, 1993)

Abstract

The small, soluble, (2Fe–2S)-containing protein ferredoxin (Fd) mediates electron transfer from the chloroplast photosystem I to ferredoxin:NADP$^+$ oxidoreductase (FNR), a flavoenzyme located on the stromal side of the thylakoid membrane. Ferredoxin and FNR form a 1:1 complex, which is stabilized by electrostatic interactions between acidic residues of Fd and basic residues of FNR. We have used differential chemical modification of Fd to locate aspartic and glutamic acid residues at the intermolecular interface of the Fd:FNR complex (both proteins from spinach). Carboxyl groups of free and FNR-bound Fd were amidated with carbodiimide/2-aminoethane sulfonic acid (taurine). The differential reactivity of carboxyl groups was assessed by double isotope labeling. Residues protected in the Fd:FNR complex were D-26, E-29, E-30, D-34, D-65, and D-66. The protected residues belong to two domains of negative electrostatic surface potential on either side of the iron–sulfur cluster. The negative end of the molecular dipole moment vector of Fd (377 Debye) is close to the iron–sulfur cluster, in the center of the area demarcated by the protected carboxyl groups. The molecular dipole moment and the asymmetric surface potential may help to orient Fd in the reaction with FNR. In support, we find complementary domains of positive electrostatic potential on either side of the FAD redox center of FNR. The results allow a binding model for the Fd:FNR complex to be constructed.

Keywords: carboxyl groups; chemical modification; dipole moment; electrostatic potential; ferredoxin; ferredoxin:NADP$^+$ oxidoreductase

The iron–sulfur protein ferredoxin plays a crucial role in the transport of electrons in chloroplasts of higher plants and algae as well as in cyanobacteria. Fd mediates electron transfer between photosystem I and the flavoenzyme ferredoxin:NADP$^+$ oxidoreductase (EC 1.18.1.2). FNR catalyzes the terminal step of the photosynthetic electron flow, the reduction of NADP$^+$ (review by Knaff & Hirasawa [1991]). Apart from being an electron donor to FNR, Fd also serves as electron donor to other chloroplast enzymes like Fd-thioredoxin reductase, nitrite reductase, and glutamate synthase (Knaff & Hirasawa, 1991). Plant Fds are soluble monomeric proteins that contain a single (2Fe–2S) cluster. They are low-potential one-electron carriers located in the stromal space of thylakoids. The proteins typically contain 93–98 residues (Matsubara & Hase, 1983).

Fd donates one electron at a time to the FAD redox center of FNR. The latter is a two-electron donor (hydride ion) to NADP$^+$. This change from a one-electron to a two-electron transfer step typically occurs in photosynthesis and respiration, as well as during biodegradation processes. In-

Reprint requests to: Hans R. Bosshard, Biochemisches Institut der Universität, Winterthurerstr. 190, CH-8057 Zürich, Switzerland.

Abbreviations: ATZ, anilinothiazolinone; CMC, 1-cyclohexyl-3-(2-morpholinyl-4-ethyl) carbodiimide; EDC, 1-ethyl-3-(3-dimethylaminopropyl) carbodiimide; Fd, ferredoxin; Fd:FNR, noncovalent complex (1:1) of Fd and FNR; FNR, ferredoxin:NADP$^+$ oxidoreductase; FPLC, fast-performance liquid chromatography; HPLC, high-performance liquid chromatography; PDR, phthalate dioxygenase reductase; PTH, phenylthiohydantoin; SDS, sodium dodecyl sulfate; taurine, 2-aminoethane sulfonic acid; TPCK, tosyl-L-phenylalanine chloromethyl ketone.

terestingly, the switch from one- to two-electron transfer has been solved in two different ways: by bringing together separate electron transfer proteins such as Fd and FNR in chloroplasts, or cytochrome *c* and cytochrome oxidase in mitochondria, or by evolutionary fusion of one- and two-electron redox centers in a single enzyme, as in phthalate dioxygenase reductase from *Pseudomonas cepacia* (Corell et al., 1992). In the case of Fd and FNR from chloroplasts, a fit between the FAD and the iron–sulfur cluster conducive to electron transfer must be created by specific association of the two proteins. In contrast, the FMN and iron–sulfur prosthetic groups of PDR are brought together by the folding of the 36-kDa polypeptide chain of this enzyme.

Fd and FNR form a tight 1:1 complex stabilized by electrostatic interactions to which Fd seems to contribute mainly negative charges (Foust et al., 1969; Batie & Kamin, 1981; Davis, 1990). When carboxyl groups of Fd were amidated with glycine ethylester, modification of only a few residues resulted in a large drop of the rate of NADP$^+$ photoreduction (Vieira & Davis, 1986), which could be attributed to a decrease in the strength of the association of the two proteins (Davis, 1990). Because the most easily modified carboxyl groups occurred in the acidic regions 26–30, 65–70, and 92–94, these regions were thought to provide negative charges for binding to FNR (Vieira & Davis, 1986; Vieira et al., 1986). Covalent cross-linking of Fd to FNR by reaction with a water-soluble carbodiimide produced cross-links to the sequence 92–94, and possibly to residues 20, 21, or 26 (Zanetti et al., 1984, 1988). NMR spectroscopy of ^{13}C-enriched Fd from *Anabaena variabilis* indicated that at least three glutamate residues are at or near the contact region between Fd and FNR (Chan et al., 1983).

In the present work, we have tried to identify glutamate and aspartate residues at the binding site of Fd for FNR (both proteins from spinach) by a differential protection technique (Bosshard, 1979, 1993). Free Fd and Fd:FNR complex were reacted with carbodiimide/taurine. Six carboxyl groups that were less reactive in the binary complex have been identified. Calculation of the molecular dipole moment and the electrostatic surface potential of Fd revealed that the protected residues are located in domains of negative potential flanking the iron–sulfur cluster on two sides. Similar calculations for FNR disclosed surface areas of positive potential on two sides of the FAD redox center. A binding model for the Fd:FNR complex is presented.

Results

Modification of carboxyl groups

Amidation of protein carboxyl groups proceeds by two steps. First, the protonated group is activated to the *O*-acylisourea derivative by reaction with a carbodiimide. This then reacts with an amine to yield the amidated protein. In separate, parallel experiments 70 μM Fd:FNR complex and 70 μM free Fd, respectively, were reacted with carbodiimide and taurine. In the following, we call "experiment B" the modification of bound Fd in the Fd:FNR complex, and "experiment F" the modification of free Fd. At the chosen reaction conditions of experiment B (25 mM ionic strength), the Fd:FNR complex was less than 5% dissociated, as tested by difference absorption spectroscopy (data not shown; Foust et al., 1969). The stability of the complex agrees with a dissociation constant below 1 μM at 25 mM ionic strength (Batie & Kamin, 1981). To keep the reaction conditions as similar as possible, the ratio of total protein carboxyl groups to carbodiimide to taurine was fixed at 1:1:1.1 in experiments B and F. In experiment B, [^{3}H]taurine was used to modify Fd, and in the parallel experiment F, [^{14}C]taurine was used. Isotope labeling was kept well below 1 taurine/Fd. This ensured that modification of one carboxyl group did not influence modification of a neighboring group. Reaction products from experiment B and F were mixed after the reaction with radiolabeled taurine. In this way it was possible to measure different degrees of carboxyl modification from the ^{14}C/^{3}H ratio of modified residues.

Two different carbodiimides were used in two sets of independent experiments, namely EDC and CMC. Treatment of the complex with carbodiimide also produces covalently cross-linked proteins (Zanetti et al., 1984; Colvert & Davis, 1988). Cross-linking can be suppressed by adding taurine in large excess over carbodiimide. Because of the high cost of radiolabeled taurine, this approach could not be taken, and taurine-modified Fd had to be separated from cross-linked reaction products. Figure 1 shows the elution profile of the chromatographic separation of the combined reaction products of experiments B and F. The composition of the cross-linked complexes, containing 50% or more of the initial Fd added, was deduced from the visible and near-UV absorption spectra and by SDS–polyacrylamide electrophoresis (not shown).

The double-labeled, purified Fd derivative was modified with excess nonradioactive taurine. Modification with excess reagent produced a derivative that still contained 20–25% unmodified carboxyl groups. The likely reason for incomplete modification was that some *O*-acylisourea derivative rearranged to the stable *N*-acylurea derivative.

Identification of modified carboxyl groups

Modified Fd was digested consecutively with trypsin and chymotrypsin and the peptides were separated by reversed-phase HPLC (Figs. 2, 3). Taurine-modified peptides had a tendency to adsorb to the octadecylsilane matrix of the reversed-phase column, resulting in broad peaks and low resolution. Only by shortening peptides through double digestion with trypsin and chymotryp-

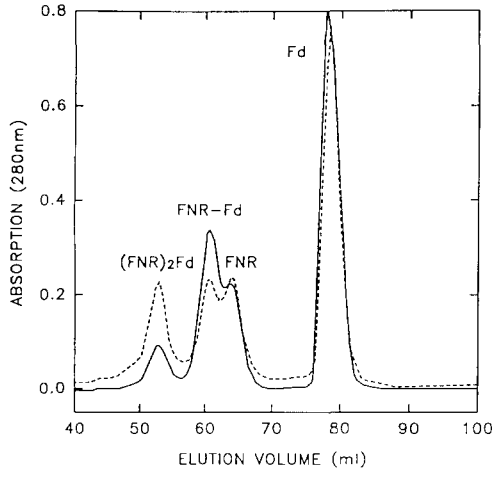

Fig. 1. Separation of products from the reaction of Fd and the Fd:FNR complex with EDC/taurine (solid line) and CMC/taurine (dotted line). Separation on a Superdex 75 (16/60) gel filtration column (Pharmacia FPLC) eluted with 0.2 M $NaKP_i$, pH 7.7 (0.5 mL/min). Samples contained 60 nmol Fd from experiments F and B, 33 nmol FNR from experiment B, and 140 nmol unmodified carrier Fd.

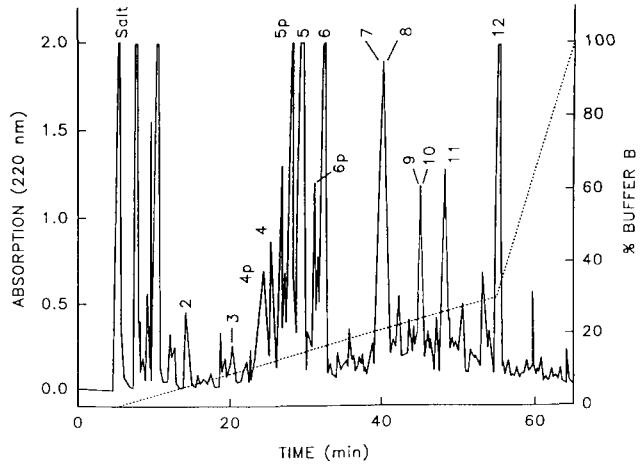

Fig. 3. Separation of tryptic/chymotryptic peptides from Fd that had been modified with CMC/taurine. Chromatography on reversed phase C_{18} column (Nucleosil 100-5C_{18}PPN, Macherey and Nagel). Binary gradient as in Figure 2. Sequences of peptides 2–9 as in Figure 2; 10, ^{53}TGSLNQDDQSF^{63}; 11, ^{24}ILDAAEEEGIDLPY^{37}; 12, ^{76}TCAAYP VSDVTIETHK^{91}.

sin have we been able to achieve good separations. All the peaks shown in Figures 2 and 3 were pooled and rechromatographed for amino acid and sequence analysis. Numbered peaks in Figures 2 and 3 account for all peptides containing Asp and Glu. Peptides in peaks 4p and 4, 5p and 5, 6p and 6 (Fig. 3) had identical amino acid compositions but differed in the extent of taurine modification. Corresponding peaks were pooled for determination of protection factors.

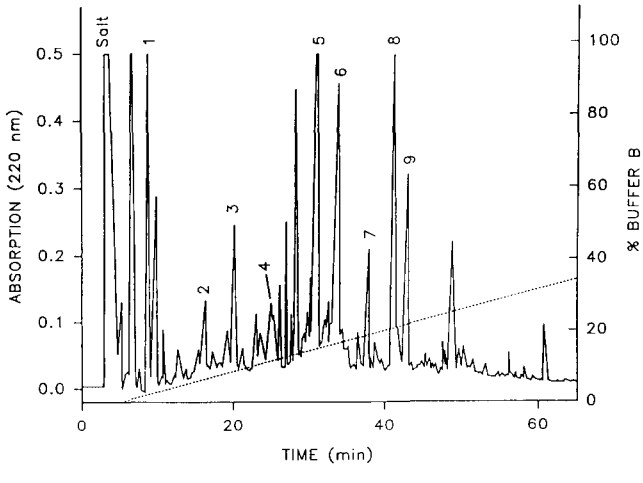

Fig. 2. Separation of tryptic/chymotryptic peptides from Fd that had been modified with EDC/taurine. Chromatography on reversed-phase C_{18} column (Nucleosil 100-5C_{18}AB, Macherey and Nagel, Düren, Germany). Elution (0.7 mL/min) with binary gradient of buffer A (3 vol % acetonitrile in 10 mM acetic acid/triethanolamine, pH 5.7) and buffer B (60 vol % acetonitrile in 10 mM acetic acid/triethanolamine, pH 5.7). 1, ^{87}IETH^{90}; 2, ^{92}EEEL^{95}; 3, ^{57}NQDDQSF^{63}; 4, ^{17}QCPDDVY^{23}; 5, ^{65}DDDQIDEGW^{73}; 6, ^{64}LDDDQIDEGW^{73}; 7, ^{78}AAYPVSDV^{85}; 8, ^{26}DAAEEEGIDLPY^{37}; 9, ^{8}VTPTGNVEF^{16}.

When sequencing the taurine-modified peptides, we found that the ATZ and PTH derivatives of modified Asp and Glu were too polar to be separated from the remaining peptide by organic solvent extraction, the procedure used in the standard automated sequencing protocol. We had to resort to solid-phase Edman degradation of the peptides coupled to aminopropyl glass. In this way, the polar ATZ derivatives could be extracted with methanol in high yield.

Determination of protection factors

To assess the differential degree of modification, a protection factor was defined as the $^{14}C/^{3}H$ ratio of each modified carboxyl group (Bosshard et al., 1987). The ratios were determined at the level of the ATZ derivatives of Asp and Glu. Protection factors were obtained for 16 of the 19 acidic residues of Fd. (Labeling of E-15, D-84, and E-88 was too weak for calculation of protection factors.) The median of the 16 protection factors was 0.50 in the experiment with EDC/taurine. The value is in reasonable agreement with the overall protection factor of 0.59 calculated for the intact modified Fd. In the experiment with CMC/taurine, the 16 residues had a median protection factor of 0.20; that of the intact labeled protein was 0.24. Considering that the specific radioactivity of [^{3}H]taurine was 6.8-fold higher than that of [^{14}C]taurine (see Materials and methods), the overall protection factors of 0.59 and 0.2 in the EDC and CMC experiment, respectively, indicate that carboxyl groups of free Fd were more reactive. The likely reason is that most of the resi-

dues found to be protected in the Fd:FNR complex (see below) were highly reactive in free Fd. Clustered acidic residues, as those identified at the binding site for FNR in the present study, are known to be more reactive (Geren et al., 1984).

To normalize the values from the two sets of experiments, each protection factor was divided by the median of all the protection factors. Normalized protection factors are shown in Table 1. Values were significantly higher for E-29, E-30, D-34, and D-65 in both the EDC and the CMC experiment. Hence, these residues were clearly protected in the Fd:FNR complex. Weaker, yet probably significant, protection was seen for D-26 and D-66. Averaging the protection factors of both experiments yielded six values higher than 1.65 (boldface numbers in Table 1), whereas the remaining 11 values were ≤1.15.

Table 1. *Protection factors*

Residue	Normalized protection factors[a]			
	EDC[b]	CMC[b]	Mean EDC + CMC[c]	Peptide[d]
D-20	0.44	0.76	0.60	4
D-21	0.40	0.76	0.58	4
D-26	1.66	1.94	**1.80**	8
E-29	3.56	6.02	**4.79**	8, 11
E-30	2.07	5.21	**3.64**	8, 11
E-31	0.99	0.42	0.71	8, 11
D-34	3.56	5.49	**4.53**	8, 11
D-59	0.44	1.50	0.97	3, 10
D-60	1.21	1.10	1.15	3, 10
D-65	15.72	5.00	**10.36**	5, 6
D-66	1.03	2.28	**1.66**	5, 6
D-67	1.00	1.02	1.01	5, 6
D-70	0.16	0.25	0.21	5, 6
E-71	0.36	0.45	0.41	5, 6
E-92	1.01	0.62	0.82	2
E-93	0.67	0.58	0.63	2
E-94	0.55	0.59	0.57	2

[a] Normalized $^{14}C/^{3}H$ ratio of protected residues; see text for calculation of normalized protection factors. The mean value is shown for residues that were analyzed in two different peptides.
[b] Values for modification with EDC/taurine and CMC/taurine, respectively.
[c] Mean of columns 2 and 3. Six means (in boldface) were higher than 1.65.
[d] See Figures 2 and 3 for numbering of peptides.

Location of protected residues in the three-dimensional structure of Fd

Figure 4 and Kinemage 1 show the molecule with the iron-sulfur cluster facing the viewer. The six residues with protection factors >1.65 (Table 1, column 4) are located on the same face of the molecule, namely D-26, E-29, E-30, and D-34 to the left of the iron-sulfur cluster, and D-65 and D-66 to the right. Also shown are residues that may cross-link to FNR in a covalent Fd:FNR complex (Zanetti et al., 1988; see Discussion).

Molecular dipole moments and electrostatic potential fields

The distribution of charged residues of Fd is asymmetric. The oxidized molecule (both irons in the ferric form) has a dipole moment of 377 Debye (1.25×10^{-27} coulomb·m). The dipole moment was calculated based on the structure obtained by fitting the spinach sequence to the *A. sacrum* structure. The dipole is indicated by a straight line in Figure 4 (see Kinemage 1). The negative end of the dipole moment vector is near S-43, close to the iron-sulfur cluster and the strongly protected residue D-65. Fd:NADP⁺ oxidoreductase also has an asymmetric charge distribution leading to a dipole moment of 558 Debye (Jelesarov et al., 1993). The positive end of the dipole moment of FNR is indicated by a star in stereo pair B of Figure 5 (see also Kinemage 2).

Electrostatic potential fields around Fd and FNR were calculated with the help of the program DelPhi. This program uses a macroscopic approach for the description of the solvent-protein dielectric boundary. The protein is treated as a low dielectric cavity immersed in a high dielectric solvent. The results of the potential calculations are shown in Figure 5. We have also calculated the electrostatic potentials of Fds from *A. variabilis* (Rypniew-

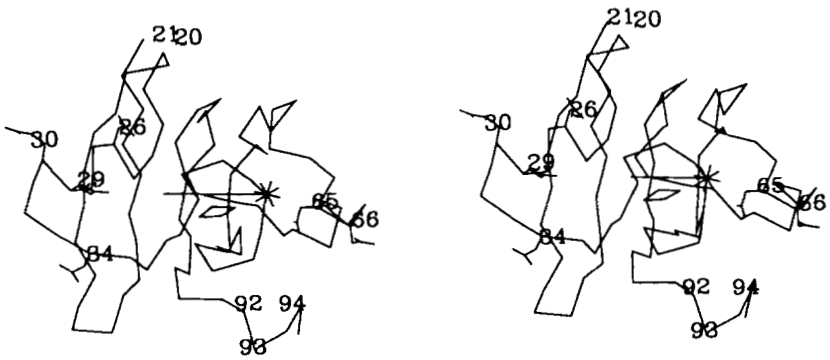

Fig. 4. Stereo model of C_α trace of Fd from *Aphanothece sacrum* to which the sequence of spinach Fd was fit. The (2Fe-2S) cluster is indicated by an oblong. Side chains of residues protected in the Fd:FNR complex are shown. Other numbered positions are of residues that were cross-linked to FNR in a covalent Fd:FNR complex (Zanetti et al., 1988; see Discussion). The molecular dipole moment vector is indicated by a straight line with the negative pole marked by an asterisk. The dipole vector is nearly perpendicular to the plane of the figure.

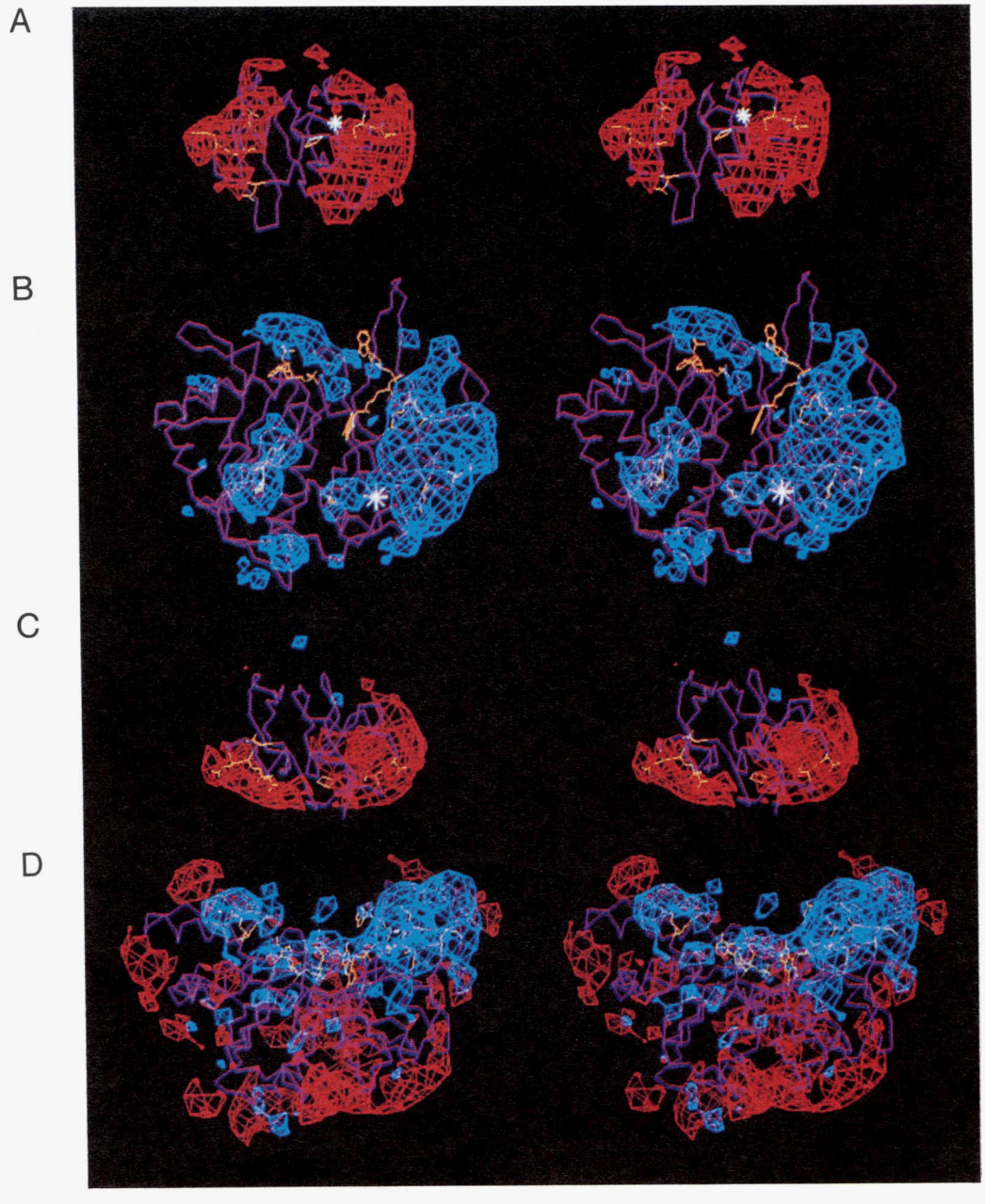

Fig. 5. Stereo models of Fd and FNR with negative (red contours) and positive (blue contours) electrostatic surface potentials. **A:** Negative potential (−15 kJ/mol) of Fd. Molecule oriented as in Figure 4. Protected residues in yellow: D-26, E-29, E-30, and D-34 in left potential domain, D-65 and D-66 in right potential domain. Negative end of dipole moment vector indicated by white asterisk. **B:** Positive potential (+5 kJ/mol) of FNR. Shown in yellow: FAD with isoalloxazine ring in central cleft; 2′-phospho-AMP in binding site for NADP (top left); K-304 and K-305 in potential domain at lower left; K-33, K-35, K-91, R-93, and K-153 in potential domain at lower right. Positive end of dipole moment vector marked by white asterisk. **C, D:** Negative and positive potentials of Fd (−15 kJ/mol and +5 kJ/mol) and FNR (−5 kJ/mol and +5 kJ/mol). The two molecules are shown approaching each other to form the Fd:FNR complex. The complementary superposition of the electrostatic potential fields at the proposed binding sites is clearly seen in this view. To obtain the views in C and D, stereo pair A was rotated counterclockwise and stereo pair B was rotated clockwise, both by 90° around a horizontal axis in the plane of the figure.

ski et al., 1991) and *Spirulina platensis* (Tsukihara et al., 1981). A very similar asymmetric and bilobal potential distribution was observed (not shown).

Electrostatic potentials depend on ionic strength. The results shown in Figure 5 are for the conditions of the modification experiment, i.e., 25 mM ionic strength and neutral pH. Qualitatively similar results were obtained at physiological ionic strength of 150 mM (not shown). A more detailed analysis of the electrostatic potentials of Fd and FNR and their dependency on ionic strength will be

the subject of another communication (I. Jelesarov, in prep.).

Discussion

Differential reactivity of carboxyl groups

Differential chemical modification has been used to map amino acid residues at contact sites of protein-protein complexes (examples by Pettigrew, 1978; Rieder & Bosshard, 1980; Bechtold & Bosshard, 1985; Hitchcock-DeGregori et al., 1985; Bosshard et al., 1987; Burnens et al., 1987; Omen & Kaplan, 1987; Wei et al., 1988). The danger that chemical modification of one residue might influence the reactivity of neighboring residues was overcome by the use of only a trace amount of the radioactive modifying reagent (Bosshard, 1979, 1993). Though this ensures that any differential modification is caused by complex formation proper, protection alone cannot prove unequivocally that a residue is part of the contact site. Occasionally, complex formation may affect chemical reactivity through conformational change(s) outside of the contact site. In the present case, the protected carboxyl groups are located in two patches on a common face of the molecule (Fig. 4; Kinemage 1). This strengthens the assumption that the protected residues are at, or close to, the FNR binding site. In addition, it is reasonable to assume that the iron-sulfur cluster is at the center of the FNR binding site. The relationship between the residues' location, the orientation of the molecular dipole moment, and the distribution of the electrostatic surface potentials of Fd and FNR further support a binding site that is demarcated by the protected carboxyl groups. This will be discussed below.

The acidic tripeptide ^{92}EEE^{94} was not protected. These residues reacted strongly with carbodiimide/glycine ethylester and were thought to be important for FNR binding (Vieira et al., 1986). Zanetti et al. (1988) found residues 92–94, and possibly one or more of aspartic acid residues 20, 21, and 26, to cross-link to FNR when the complex was treated with EDC. However, of these cross-linked residues, only D-26 was weakly protected in the present experiment. We believe cross-linking is less likely to take place at the very binding site for FNR because to cross-link, EDC must have easy access to carboxyl groups. Therefore, the cross-linking data are complementary to the present results. In the view of Fd presented in Figure 4 and Kinemage 1, the cross-linked residues are below and above the iron-sulfur cluster.

Residues D-70 and D-71 had low protection factors (Table 1), indicating that these residues were somewhat more reactive in the FNR-bound Fd. Residues D-70 and D-71 face toward the backside of the molecule (Fig. 4; Kinemage 1). A small conformational change could increase chemical reactivity, for example by decreasing the pK_a of the carboxyl groups (Bosshard, 1979).

Molecular dipole moment and electrostatic surface potential distribution

In stereo pair A of Figure 5 (see also Kinemage 1), the two domains of negative potential on either side of the iron-sulfur cluster of Fd spring to the eye. The left domain contains protected residues D-26, E-29, E-30, and D-34. Protected residues D-65 and D-66 are in the right domain. Between these domains and just above the iron-sulfur cluster is the negative end of the molecular dipole. We believe this orientation of the dipole is not coincidental. A dipole moment centered at the binding site for electron donors and acceptors was observed in cytochrome *c* (Koppenol & Margoliash, 1982; Rush & Koppenol, 1987; Koppenol et al., 1991) and in plastocyanin (Rush et al., 1988). There is evidence that in these cases the dipole moment helps to steer the proteins into proper orientation on the surface of redox partners.

The potential distribution and dipole moment orientation of Fd immediately suggests the existence of a complementary pattern at the binding site of FNR. Such a pattern was found, as shown by stereo pair B of Figure 5 (see also Kinemage 2). There is a region of positive potential containing K-304 and K-305 to the lower left of the interdomain cleft of FNR where the planar isoalloxazine ring of FAD approaches the molecular surface. To the right of the FAD cleft is a larger positive domain with K-33, K-35, K-91, and R-93. An arm of the right domain extends toward the lower center of the molecule; K-153 and the positive end of the molecular dipole of FNR are in this arm. A third domain of positive potential is in the region of the NADP$^+$ binding site (top of molecule as oriented in stereo pair B). This domain is more toward the back of the molecule and does not belong to the proposed binding site for Fd.

In stereo pairs C and D of Figure 5 (see also Kinemage 3), a complementary fit is evident between the domains of negative and positive surface potential of Fd and FNR, respectively. The negative domain of Fd with D-26, E-29, E-30, and D-34 of Fd matches to the positive domain of FNR with K-304 and K-305. Similarly, the negative domain of Fd with D-65 and D-66 matches to the positive domain of FNR with K-33, K-35, K-91, and R-93. Juxtaposition of the charged surface domains brings the iron-sulfur cluster immediately above the FAD prosthetic group. The most exposed edge of the iron-sulfur cluster may approach the exposed dimethylbenzyl ring of FAD to within a few Ångstroms without having other parts of the molecule "bump" into each other (not shown). As a control, modeling was also performed using the structure of *Anabaena* Fd to which the spinach sequence was adapted. Essentially the same superposition of negative and positive electrostatic potentials containing the same acidic and basic residues as in the *Aphanothece* Fd/spinach FNR model was seen (not shown).

An Fd binding site demarcated by the positive poten-

tial domains adjacent to the FAD prosthetic group is supported by independent chemical modification studies of Fd:FNR complexes. In the larger domain on the right (Fig. 5, stereo pair B; Kinemage 2), K-33, K-35, and K-153 were protected from chemical modification by lysine specific reagents in the spinach Fd:FNR complex (Jelesarov et al., 1993). In FNR from *Anabaena* sp. PCC 7119, R-77 and K-294 were protected from chemical modification in the presence of Fd from *Anabaena* (Medina et al., 1992a,b). The protected residues correspond to R-93 and K-305 in the right and left potential domain, respectively, of spinach FNR.

After the present work had been completed, the crystal structure of PDR was published (Corell et al., 1992). FMN and (2Fe-2S) redox centers are combined within the single polypeptide chain of this enzyme. The PDR catalyzes a reaction analogous to that taking place between Fd and FNR. The folding of the FAD, the NAD^+ binding, and the iron-sulfur cluster domains of PDR are very similar to the folding of the FAD and the $NADP^+$ binding domains in plant FNR and to the folding of cyanobacterial Fd, respectively. However, the amino acid sequence similarity between PDR and FNR/Fd is less than 20% (Corell et al., 1992). The iron-sulfur and FMN prosthetic groups of PDR approach each other to within 4.9 Å between the 8-methyl group of FMN and a cysteine-sulfur ligated to one of the irons of the (2Fe-2S) cluster. The interaction model for the Fd:FNR complex we are proposing here is surprisingly similar to the structure of the interdomain contact between the FMN domain and the iron-sulfur domain of crystalline PDR. Similar electron transfer conduits are achieved by association of Fd and FNR and by the folding of the polypeptide chain of PDR. However, the acidic and basic residues deduced from our modification experiments (this work and Jelesarov et al. [1993]) are missing in the PDR structure.

We envisage the following mechanism of complex formation between Fd and FNR. First, the two molecules are steered toward each other through the complementary orientation of the strong molecular dipole moments. This brings the two molecules into an approximately correct orientation. Second, the complementary electrostatic surface potentials guide the molecules to optimally orient the redox prosthetic groups. Charge-charge interactions between basic residues of FNR and acidic residues of Fd may help attain the optimal orientation. However, such bonds may not contribute strongly to the energy of binding at physiological ionic strength and need not be essential for electrostatic interaction. The mechanism envisaged will increase the percentage of productive encounter complexes, in agreement with kinetic studies (Walker et al., 1991).

The resolution of our model is not as high as might be expected given the high resolution of the X-ray structures we have used. A more precise docking model can be built in which the prosthetic groups of Fd and FNR approach each other to within less than 4 Å and in which some of the protected acidic residues of Fd come within ionic bond distance to some of the protected basic residues of FNR (I. Jelesarov, unpubl.). We are reluctant to attach much significance to such a "high-resolution" docking complex. First, our model building uses a cyanobacterial Fd structure into which the spinach sequence was fit. Second and more important, in the case of protein-protein complexes of known structure, the actual structure could not be predicted unequivocally even by a most elaborate docking procedure (Walls & Sternberg, 1992). Similarly, the X-ray analysis of a crystalline complex of cytochrome *c* with cytochrome *c* peroxidase turned out to differ significantly from a docking model thought to be well founded (Pelletier & Kraut, 1992). Finally, there is increasing evidence for the idea that electron transfer proteins are built to facilitate more than just a single intermolecular electron transfer pathway (Northrup et al., 1988; Burch et al., 1990; Roberts et al., 1991; Bosshard, 1993). In the present case, Fd and FNR may be free to move against each other about the surface domains characterized and outlined in the present work. We believe such a "rolling ball" mechanism may be a more appropriate description of the Fd:FNR electron transfer complex than a static picture modeled along the lines of an enzyme:substrate complex.

Materials and methods

Fd and FNR were isolated from spinach leaves following published procedures (Tagawa & Arnon, 1968; Shin & Oshino, 1978). Isoform I of Fd (Ohmori et al., 1989) was used in all experiments. Concentrations of FNR and Fd were determined using extinction coefficients ($M^{-1}cm^{-1}$) of 9,680 at 420 nm for Fd (Tagawa & Arnon, 1968) and 10,740 at 460 nm for FNR (Forti et al., 1970).

Modification with radioactive taurine

Experiment B

Fd (630 nmol modifiable carboxyl groups), FNR (1,520 nmol modifiable carboxyl groups), and [^{3}H]taurine (2,360 nmol, 8.14 GBq/mmol; Amersham) were incubated in 10 mM $NaKP_i$, pH 7.2, at room temperature during 15 min. The reaction was started by adding EDC (2,150 nmol). The final concentrations in a total reaction volume of 0.42 mL were Fd = 70 μM, FNR = 78 μM, [^{3}H]taurine = 5.6 mM, and EDC = 5.1 mM. The reaction was stopped after 4 h by addition of 0.1 mL of 0.5 M nonradioactive taurine in 0.2 M $NaKP_i$, 3 M NaCl, pH 7.7. Modification with CMC/taurine was performed in the same way except that 1 mM *N*-hydroxysuccinimide was included. This additive enhances the coupling reaction through the formation of an intermediary *N*-hydroxysuccinimide ester (Staros et al., 1986).

Experiment F

Fd and [^{14}C]taurine (1.2 GBq/mmol) were incubated as in experiment B, and the reaction was started by addition of EDC or CMC. Final concentrations in a reaction volume of 0.42 mL were Fd = 70 μM, [^{14}C]taurine = 1.65 mM, and carbodiimide = 1.5 mM.

Exhaustive modification of carboxyl groups

Reaction mixtures for experiments B and F, containing equimolar amounts of Fd, were mixed, and modified Fd was purified by gel filtration on Superdex 75 (Fig. 1). Carrier Fd (400 nmol) was added to the purified Fd sample and the protein was denatured in 6 M guanidinium·HCl, 50 mM $NaKP_i$, pH 8. Free SH groups of denatured Fd were carboxymethylated with iodoacetamide (Zanetti et al., 1988). The carboxymethylated Fd was brought into 0.1 M sodium cacodylate·HCl, pH 5.2, 5 M guanidinium·HCl by chromatography on a disposable gel filtration column (BioRad 10 DG). Solid taurine (Fluka) was added to a final concentration of 0.5 M, followed by solid EDC to a concentration of 20 mM. Addition of the same amount of EDC was repeated after 30, 60, and 90 min, and 8 and 16 h. After 24 h, the buffer was changed to 0.1 M NH_4HCO_3 by gel filtration (BioRad 10 DG). The amount of incorporated taurine was measured by amino acid analysis.

Digestion of modified Fd and separation of peptides

Modified, carboxymethylated Fd in 0.1 M NH_4HCO_3 was digested at 37 °C with a total of 4% (w/w) of trypsin (Fluka, TPCK treated) added in four aliquots over a period of 24 h. The solution was made 0.1 mM in $CaCl_2$ and chymotrypsin (Fluka) was added to a final concentration of 2% (w/w), added in two aliquots over a period of 8 h. Peptides were separated by reversed-phase HPLC, as described in the legends to Figures 2 and 3. Some peptides could be separated only by rechromatography using a more shallow gradient than indicated in Figures 2 and 3.

Solid-phase sequencing

Dried peptides (10–100 nmol) were preincubated with anhydrous trifluoroacetic acid (Salnikow, 1986) and coupled to 3-aminopropyl glass beads (Pierce CPG/3-aminopropyl glass, 75 Å pore diameter, 37–74 μm particle size) according to the procedure of Machleidt et al. (1986). Edman degradation followed the method of Chang (1981), except that all the reaction steps were performed in Eppendorf tubes and the cleaved-off reaction products were recovered in the supernatant after pelleting of the glass beads by centrifugation. A small fraction of the ATZ derivative was converted to the PTH derivative, which was identified by HPLC. The main fraction was used for liquid scintillation counting to get the $^{14}C/^{3}H$ ratio.

Three-dimensional structure of spinach Fd

The amino acid sequence of spinach Fd, for which no crystal structure is known, was fit to the published structure of Fd from *Aphanothece sacrum* (Tsukihara et al., 1990). This structure was chosen because among the three (2Fe–2S)-containing Fds for which crystal structures are known, the sequence of the *A. sacrum* protein is the most similar to that of spinach Fd. The two proteins are 68% identical in sequence. Including conservative substitutions, sequence similarity is near 80%. There are no deletions or insertions. In the fitting process, the backbone dihedral angles were not changed. Side chains were adjusted manually to avoid bad contacts and to fit the conformation of individual residues to the statistical rotamer library (Ponder & Richards, 1987).

Computational methods

The dipole moment of Fd was calculated as described for spinach plastocyanin (Rush et al., 1988). Fd has a negative net charge and the dipole moment $\vec{\mu}$ was calculated with the help of the following equation:

$$\vec{\mu} = n(\vec{r}_P - \vec{r}_N)e + (p - n)\vec{r}_N e,$$

in which n and p are the numbers of negative and positive charges and $\vec{r}_N$ and $\vec{r}_P$ are the radius vectors from the center of mass to the center of positive and negative charge, respectively. The distance between the centers of positive and negative charge is $\vec{r}_P - \vec{r}_N$, and e is the elementary charge. It was assumed that all lysines and arginines carry a positive charge, and that all glutamic and aspartic acids are negatively charged. A positive charge was placed at the peptide N of A-1, and a negative charge at the peptide O of C-terminal A-97. The contribution of peptide bonds in the α-helix 23–32 was taken into account with the approximation of half a positive charge at the N-terminus and half a negative charge at the C-terminus (Koppenol & Margoliash, 1982). All other bond dipoles were assumed to have random orientations and were ignored. The cysteinyl sulfurs of the (2Fe–2S) cluster were assigned a single negative charge and a charge of −2 was given to the two labile sulfurs of the cluster. The two irons were assumed to be in the ferric state, charge +3. Together, Fd has 12.5 positive and 29.5 negative charges. Calculation of the dipole moment of FNR has been described elsewhere (Jelesarov et al., 1993).

Electrostatic surface potentials were calculated using the finite difference solution to the Poisson–Boltzmann equation as implemented in the program DelPhi from Biosym Technologies, San Diego, California (Gilson et al., 1988; Gilson & Honig, 1988; Klapper et al., 1986). Co-

ordinates of FNR and Fd from *Aphanothece* and *Anabaena*, to which the spinach Fd sequence was fitted, were obtained from the Brookhaven Protein Data Bank (entries FNR2, 1FXI, and 1FXA). Partial atomic charges were assigned using the consistent valence force-field potential function (Dauber-Osguthorpe et al., 1988). Charges of the (2Fe-2S) cluster were as described above for the calculation of the dipole moment. In FNR, two negative charges were assigned to oxygens of the pyrophosphate of FAD (atom numbers 2,374 and 2,378 in the PDB file). Solvent and ionic strength effects were treated in a continuum model with dielectric constants of 2 and 80 for the points inside and outside of the protein-solvent boundary (Gilson & Honig, 1986; Sharp & Honig, 1990). The grid for the finite difference calculation was chosen to leave a 10-Å border between the protein and the grid edge, resulting in a cubic lattice with 65 points per side for Fd and 80 points per side for FNR. The point spacing was typically 0.875 Å/point (Fd) and 1.0 Å/point (FNR).

Acknowledgments

We thank Robert R. Zinn for help with dipole moment calculations. We also acknowledge a helpful suggestion by one of the reviewers. M. Hirasawa and D.B. Knaff provided the proteins used in this study. This work was supported by the Swiss National Science Foundation (grant 31-30815.91 to H.R.B.), by a grant from the Council for Tobacco Research USA (to W.H.K.), and by the US National Science Foundation and the US Department of Energy (grants INT-8822574 and DE-FG05-90ER20017 to D.B.K.).

References

Batie, C.J. & Kamin, H. (1981). The relation of pH and oxidation-reduction potential to the association state of the ferredoxin:ferredoxin $NADP^+$ reductase complex. *J. Biol. Chem. 256*, 7756-7763.

Bechtold, R. & Bosshard, H.R. (1985). Structure of an electron transfer complex. II: Chemical modification of carboxyl groups of cytochrome *c* peroxidase in presence and absence of cytochrome *c*. *J. Biol. Chem. 260*, 5191-5200.

Bosshard, H.R. (1979). Mapping contact areas in protein-nucleic acid and protein-protein complexes by differential chemical modification. *Methods Biochem. Anal. 25*, 273-301.

Bosshard, H.R. (1993). Differential protection techniques in the analysis of cytochrome *c* interaction with electron transfer proteins. In *Cytochrome c Source Book* (Mauk, A.G. & Scott, R.A., Eds.), in press. University Science Press, Mill Valley, California.

Bosshard, H.R., Wynn, R.M., & Knaff, D.B. (1987). Binding site on *Rhodospirillum rubrum* cytochrome c_2 for the *Rhodospirillum rubrum* cytochrome bc_1 complex. *Biochemistry 26*, 7688-7693.

Burch, A.M., Rigby, S.E.J., Funk, W.D., MacGillivray, R.T.A., Mauk, M.R., Mauk, A.G., & Moore, G.R. (1990). NMR characterization of surface interactions in the cytochrome *b*5-cytochrome *c* complex. *Science 247*, 831-833.

Burnens, A., Demotz, S., Corradin, G., Binz, H., & Bosshard, H.R. (1987). Epitope mapping by differential chemical modification of free and antibody-bound antigen. *Science 235*, 780-783.

Chan, T.M., Ulrich, E.L., & Markley, J.L. (1983). Nuclear magnetic resonance studies of two-iron-two-sulfur ferredoxins. 4. Interactions with redox partners. *Biochemistry 22*, 6002-6007.

Chang, J.-Y. (1981). N-terminal sequence analysis of polypeptides at the picomole level. *Biochem. J. 199*, 557-564.

Colvert, K.K. & Davis, D.J. (1988). Characterization of a covalently linked complex involving ferredoxin and ferredoxin:$NADP^+$ reductase. *Photosynth. Res. 17*, 231-245.

Corell, C.C., Batie, C.J., Ballou, D.P., & Ludwig, M.L. (1992). Phthalate dioxygenase reductase: A modular structure for electron transfer from pyridine nucleotides to (2Fe-2S). *Science 258*, 1604-1610.

Dauber-Osguthorpe, P., Roberts, V.A., Osguthorpe, D.J., Wolff, J., Genest, M., & Hagler, A.T. (1988). Structure and energetics of ligand binding to proteins: *E. coli* dihydrofolate reductase-trimethoprim, a drug-receptor system. *Proteins Struct. Funct. Genet. 4*, 31-47.

Davis, D.J. (1990). Tryptophan fluorescence studies of ferredoxin:$NADP^+$ reductase indicate the presence of tryptophan in or near the ferredoxin binding site. *Arch. Biochem. Biophys. 276*, 1-5.

Forti, G., Melandri, B.A., San Pietro, A., & Ke, B. (1970). Studies on the photoreduction of ferredoxin and the ferredoxin-NADPH reductase flavoprotein by chloroplast fragments: Effect of pyrophosphate. *Arch. Biochem. Biophys. 140*, 107-112.

Foust, F.G., Mayhew, S.G., & Massey, V. (1969). Complex formation between ferredoxin triphosphopyridine nucleotide reductase and electron transfer proteins. *J. Biol. Chem. 244*, 964-970.

Geren, L.M., O'Brien, P., Stonehuerner, J., & Millett, F. (1984). Identification of specific carboxyl groups on adrenodoxin that are involved in the interaction with adrenodoxin reductase. *J. Biol. Chem. 259*, 2155-2160.

Gilson, M.K. & Honig, B. (1986). The dielectric constant of a folded protein. *Biopolymers 25*, 2097-2119.

Gilson, M.K. & Honig, B. (1988). Energetics of charge-charge interactions in proteins. *Proteins Struct. Funct. Genet. 3*, 32-52.

Gilson, M.K., Sharp, K.A., & Honig, B. (1988). Calculating the electrostatic potential of molecules in solution: Method and error assessment. *J. Comp. Chem. 9*, 327-335.

Hitchcock-DeGregori, S.E., Lewis, S.F., & Chou, T.M. (1985). Tropomyosin lysine reactivities and relationship to coiled-coil structure. *Biochemistry 24*, 3305-3314.

Jelesarov, I., De Pascalis, A.R., Koppenol, W.H., Hirasawa, M., Knaff, D.B., & Bosshard, H.R. (1993). *Eur. J. Biochem.*, in press.

Klapper, I., Hagstrom, R., Fine, R., Sharp, K.A., & Honig, B. (1986). Focussing the electric fields in the active site of Cu, Zn superoxide dismutase. *Proteins Struct. Funct. Genet. 1*, 47-79.

Knaff, D.B. & Hirasawa, M. (1991). Ferredoxin-dependent chloroplast enzymes. *Biochim. Biophys. Acta 1056*, 93-125.

Koppenol, W.H. & Margoliash, E. (1982). The asymmetric distribution of charges on the surface of horse cytochrome *c*. Functional implications. *J. Biol. Chem. 257*, 4426-4437.

Koppenol, W.H., Rush, J.D., Mills, J.D., & Margoliash, E. (1991). The dipole moment of cytochrome *c*. *Mol. Biol. Evol. 8*, 545-558.

Machleidt, W., Borchart, U., & Ritonja, A. (1986). Solid-phase microsequencing: Procedures and their potential for practical sequence analysis. In *Advanced Methods in Protein Microsequence Analysis* (Wittmann-Liebold, B., Ed.), pp. 91-107. Springer-Verlag, Berlin.

Matsubara, H. & Hase, T. (1983). Phylogenetic consideration of ferredoxin sequences in plants, particular algae. In *Proteins and Nucleic Acids in Plant Systematics* (Jensen, U. & Fairbrothers, D.E., Eds.), pp. 168-181. Springer-Verlag, Berlin.

Medina, M., Mendez, E., & Gomez-Moreno, C. (1992a). Lysine residues of ferredoxin-$NADP^{++}$ reductase from *Anabaena* sp. PCC 1719 involved in substrate binding. *FEBS Lett. 298*, 25-28.

Medina, M., Mendez, E., & Gomez-Moreno, C. (1992b). Identification of arginyl residues involved in the binding of ferredoxin-$NADP^{++}$ reductase from *Anabaena* sp. PCC 1719 to its substrates. *Arch. Biochem. Biophys. 299*, 281-286.

Northrup, S.H., Boles, J.O., & Reynolds, J.C.L. (1988). Brownian dynamics of cytochrome *c* and cytochrome *c* peroxidase association. *Science 241*, 67-70.

Ohmori, D., Hasumi, H., Yamakura, F., Murakami, M., Fujisawa, K., Taneoka, Y., & Yamamura, T. (1989). Studies on the molecular structure of spinach ferredoxin. I. Comparison of two molecular species of ferredoxin. *Biochim. Biophys. Acta 996*, 166-172.

Omen, R.P. & Kaplan, H. (1987). Competitive labeling as an approach to defining the binding surface of proteins: Binding of monomeric insulin to lipid bilayers. *Biochemistry 26*, 303-308.

Pelletier, H. & Kraut, J. (1992). Crystal structure of a complex between electron transfer partners, cytochrome *c* peroxidase and cytochrome *c*. *Science 258*, 1748-1755.

Pettigrew, G.W. (1978). Mapping an electron transfer site on cytochrome *c*. *FEBS Lett. 86*, 14–16.

Ponder, J.W. & Richards, F.M. (1987). Tertiary templates for proteins. Use of packing criteria in the enumeration of allowed sequences for different structural classes. *J. Mol. Biol. 193*, 775–791.

Rieder, R. & Bosshard, H.R. (1980). Comparison of the binding sites on cytochrome *c* for cytochrome *c* oxidase, cytochrome *c* reductase, and cytochrome *c*1. *J. Biol. Chem. 255*, 4732–4739.

Roberts, V.A., Freeman, H.C., Olson, A.J., Tainer, J.A., & Getzoff, E.D. (1991). Electrostatic orientation of the electron-transfer complex between plastocyanin and cytochrome *c*. *J. Biol. Chem. 266*, 13431–13441.

Rush, J.D. & Koppenol, W.H. (1987). Effect of a dipole moment on the ionic strength dependence of electron-transfer reactions of cytochrome *c*. *J. Am. Chem. Soc. 109*, 2679–2682.

Rush, J.D., Levine, F., & Koppenol, W.H. (1988). The electron transfer site of spinach plastocyanin. *Biochemistry 27*, 5876–5884.

Rypniewski, W.R., Breiter, O.R., Benning, M.M., Wesenberg, G., Oh, B.-M., Markley, J.L., Rayment, I., & Holden, H.M. (1991). Crystallisation and structure determination to 2.5 Å resolution of the oxidized (2Fe–2S) ferredoxin isolated from *Anabaena* 7120. *Biochemistry 30*, 4126–4131.

Salnikow, J. (1986). Automated solid-phase microsequencing using DABITC, on-column immobilisation of proteins. In *Advanced Methods in Protein Microsequence Analysis* (Wittmann-Liebold, B., Ed.), pp. 108–116. Springer-Verlag, Berlin.

Sharp, K.A. & Honig, B. (1990). Electrostatic interactions in proteins: Theory and applications. *Annu. Rev. Biophys. Biophys. Chem. 19*, 301–332.

Shin, M. & Oshino, R. (1978). Ferredoxin-Sepharose 4B as a tool for the purification of ferredoxin-NADP^{++} reductase. *J. Biochem. (Tokyo) 83*, 357–361.

Staros, J.V., Wright, R.W., & Swingle, D.M. (1986). Enhancement by *N*-hydroxysulfosuccinimide of water-soluble carbodiimide mediated coupling reactions. *Anal. Biochem. 156*, 220–222.

Tagawa, K. & Arnon, D.I. (1968). Oxidation–reduction potentials and stoichiometry of electron transfer in ferredoxins. *Biochim. Biophys. Acta 153*, 602–613.

Tsukihara, T., Fukuyama, K., Mizushima, M., Harioka, T., Kusunoki, M.O., Katsube, Y., Hase, T., & Matsubara, M. (1990). Structure of the (2Fe–2S) ferredoxin I from the blue-green algae *Aphanothece sacrum* at 2.2 Å resolution. *J. Mol. Biol. 216*, 399–410.

Tsukihara, T., Fukuyama, K., Nakamura, M., Katsube, Y., Tanaka, N., Kakudo, M., Wada, K., Hase, T., & Matsubara, M. (1981). X-ray analysis of a (2Fe–2S) ferredoxin from *Spirulina platensis*. Main chain fold and location of side chains at 2.5 Å resolution. *J. Biochem. (Tokyo) 90*, 1763–1773.

Vieira, B., Colvert, K.K., & Davis, D.J. (1986). Chemical modification and cross-linking as probes of regions of ferredoxin involved in its interaction with ferredoxin:NADP$^+$ reductase. *Biochim. Biophys. Acta 851*, 109–122.

Vieira, B. & Davis, D.J. (1986). Interaction of ferredoxin with ferredoxin:NADP$^+$ reductase: Effects of chemical modification of ferredoxin. *Arch. Biochem. Biophys. 247*, 140–146.

Walker, M.C., Pueyo, J.J., Navarro, J.A., Gómez-Moreno, C., & Tollin, G. (1991). Laser flash photolysis studies of the kinetics of reduction of ferredoxins and ferredoxin-NADP$^+$ reductases from *Anabaena* PCC 7119 and spinach: Electrostatic effects on intracomplex electron transfer. *Arch. Biochem. Biophys. 287*, 351–358.

Walls, P.H. & Sternberg, M.J.E. (1992). New algorithm to model protein–protein recognition based on surface complementarity. Application to antibody–antigen docking. *J. Mol. Biol. 228*, 277–297.

Wei, Q., Jackson, A.E., Pervaiz, S., Carraway, K.L., Lee, E.Y.C., Puett, D., & Brew, K. (1988). Effects of interaction with calcineurin on the reactivities of calmodulin lysines. *J. Biol. Chem. 263*, 19541–19544.

Zanetti, G., Aliverti, A., & Curti, B. (1984). A cross-linked complex between ferredoxin and ferredoxin-NADP$^+$ reductase. *J. Biol. Chem. 259*, 6153–6157.

Zanetti, G., Morelli, D., Ronchi, S., Negri, A., Aliverti, A., & Curti, B. (1988). Structural studies on the interaction between ferredoxin and ferredoxin-NADP$^+$ reductase. *Biochemistry 27*, 3753–3759.